*Al Azhar Bulletin of Science Vol. 29, No. 1, (June) 2018, pp. 11-29*

# NUCLEAR STAGGERING IN SUPERDEFORMED SIGNATURE PARTNERS IN A~190 REGION USING PARTICLE –ROTOR MODEL

**M.D. Okasha**

*Physics Department, Faculty of Science (Girls branch), Al-Azhar University, Cairo, Egypt.*
*E-mail: mady200315@yahoo.com*

## ABSTRACT

*Five pairs of superdeformed (SD) signature partners in the mass region A~190 namely: $^{191}$Hg (SD2, SD3), $^{193}$Hg (SD1,SD2) , $^{193}$Hg (SD3,SD4), $^{191}$Tl (SD1,SD2) and $^{193}$Tl (SD1,SD2) are studied in version of particle – rotor model. We considered the odd-A nucleus as a system of three valence particles coupled to an even- even symmetric deformed core. The three extra core particles lie in high- j intruder orbital and occupy only two Nilsson levels with $|\Omega_1| = 1/2$ and $|\Omega_2| = 3/2$. There are four completely antisymmetric functions with K = $\pm 1/2$ and K = $\pm 3/2$ and only two basis functions . We diagonalized the $2\times2$ matrix of the total Hamiltonian and evaluated the excitation energies . Transition energies $E_\gamma$, rotational frequencies $\hbar\omega$ , dynamic $J^{(2)}$ and kinematic $J^{(1)}$moments of inertia have been calculated . A very good agreement with the experimental data support the proposed model by calculating the $\chi^2$. The bands exhibit the usual increasing of $J^{(2)}$ with $\hbar\,\omega$.*

*The $\Delta I = 1$ energy staggering in $\gamma$- ray transition energies presented in these odd- A SD nuclei has been examined by proposing a two staggering functions: the first one depending on the dipole transitions linking the two signature partners and the quadrupole transitions within each band and the second one depending only on the dipole transition energies linking the two signature partners. Our selected signature partners in Hg and Tl nuclei show large amplitude staggering pattern.*

## 1.INTRODUCTION

Over the past decade, the study of superdeformation has occupied one of the most remarkable discoveries in the nuclear spectroscopy .Since the discovery of first high spin superdeformed(SD) band in $^{152}$Dy[ 1] ,hundreds of SD states have been recognized in several mass regions A~ 60,80, 130, 150, 190 [ 2,3].Every region of super-deformation possesses its characteristics, so systematic investigations on similarities and differences among the SD bands in the different mass regions are needed for a deeper understanding of SD structure .In mass regions A~ 130 and 150, the SD structure roughly correspond to a prolate nuclear shape with a major –to minor axis ratio of 3:2:2 and 2:1:1 respectively .The quadrupole moment measurements for A~ 190 region have shown a deformation which gives a shape intermediate between A~ 130 and A~ 150 and the $\beta_2$value around 0.4.The dynamical moment of inertia $J^{(2)}$ behaves so differently for different regions of SD nuclei ,for A~ 190 all SD bands have similar values of $J^{(2)}$ , which typically increases smoothly as rotational frequency increases. This rise in $J^{(2)}$ results from the alignment of the angular momenta of paired nucleons in high- j low $\Omega$ intruder orbital and from the gradual disappearance of pairing correlation with collective rotation [ 4,5] .For A~ 150 , however , $J^{(2)}$ mostly decreases with a great deal of variation from nucleus to nucleus.

Several experimental[ 6-9] and theoretical [ 10-13] efforts have been devoted to explains the nature of SD shapes in nuclei. Theoretically , among their efforts are the cranked Nilsson –Strutinsky approach based on Woods- Saxon potential [14,15], self consistent cranked Hartree- Fock-Bogoliubov approaches based either on Skyrme type [ 15-18] or with finite range forces of Gogny type [ 19-21], relativistic Hartree -Bogoliubov approach with Gogny force[ 22] , generator coordinate method with Gogny force [ 23] and projected shell model with the quadrupole pairing[ 24].

The cascades of the SD bands .which are often unusually long, are connected by electric quadrupole transitions. However, the spin assignments and the exact excitation energies of most of these SD bands remain unknown . This is because of the absence information on linking transitions to levels of normally deformation (ND) except in few cases. Several theoretical approaches to predict the spins of SD rotational bands were proposed[ 25-29]. In our previous publications [ 29-39] , we have used some simple collective models like Bohr- Mottelson (I+1)expansion, Harris $\omega^2$ expansion, a b and a b c empirical formulas and variable moment of inertia to determine the bandhead spins in A~60,80, 150,190 mass regions.

It was found that many SD bands observed in odd-A nuclei in the A~190 region are signature partner SD bands[ 40-43]. Most of these signature partners show large amplitude staggering and the bandhead moments of inertia of each pair are almost identical .This dipole transition $\Delta I = 1$ staggering was investigated by using different staggering indices like the staggering index which represent the difference between the average transitions $I+2 \to I$ and $I \to I-2$ energies in one band and the transition $I+1 \to I-1$energies in the signature partner[ 44-51].

The plain of the paper is as follows, we used the Nilsson-plus Particle Rotor Model (PRM) to describe the superdeformed rotational bands (SDRB's). Then we study the systematic behavior of kinematic $J^{(1)}$and dynamic $J^{(2)}$ moments of inertia as a function of rotational frequency. The results are used in a description of $\Delta I=1$ energy staggering in five pairs of signature partners of Hg and Tl odd-A, by using two proposed signature functions.

## 2. Outline of The Model

In the particle rotor model (PRM) considered here, the odd-A superdeformed nucleus is assumed to consist of a deformed axially symmetric core of even- even numbers of nucleons plus three valence particles occupying high two Nilsson levels with $|\Omega_1| = 1/2$ and $|\Omega_2| = 3/2$ and coupled to the core. Since the excitation energy spectrum of the core is very difficult to simulate through any simple energy angular momentum relationship, we use the variable moment of inertia (VMI) core formalism. The Hamiltonian is given by

$$H_p = \sum_{i=1}^{3}\left[\frac{-\hbar^2}{2m_i}\nabla_i^2 + V_{Nilsson}(r_i)\right] + \sum_{i=1}^{3}\frac{R_i^2}{2\theta_I} + \frac{C}{2}(\theta_I - \theta)^2 \quad (1)$$

Where $\theta_I$ are the components of moments of inertia parameter describing the quadruple deformation , $R_i$ are the components of the core angular moments R with respect to body fixed frame, $\hat{R} = \hat{I} - \hat{J}$ with I is the total angular momentum of the nucleus and J is the total angular momentum of the valance particles

$$J = \sum_{i=1}^{3} j_i \qquad (2)$$

For an axially symmetric rotor , the component $R_3$ along the symmetry axis 3 is a constant of motion and it is assumed that $R_3=I_3-J_3=0$

Let us introduce the raising and lowering operators such that

$$I^{(\pm)} = I_1 \pm iI_2 \quad , \quad J^{(\pm)} = j_1 \pm ij_2 \qquad (3)$$

The Hamiltonian of equation (1) may be written as

$$H = H_A + H_{PR} + H_P + H_j + H_{PPC} \qquad (4)$$

The different parts of the Hamiltonian of equation (4) may be interpreted as rotational Hamiltonian $H_A$, particle rotor coupling term $H_{PRC}$ , single- particle Hamiltonian ($H_P$+$Hj$) and the particle- particle coupling term $H_{PPC}$ they are given by

$$H_A = \frac{1}{2\theta}(I^2 - I_3^2) + \frac{C}{2}(\theta_I - \theta)^2 \qquad (5)$$

$$H_{PRC} = \frac{-1}{2\theta}\left[I^{(+)}\sum_{i=1}^{3} j^{(-)}(i) + I^{(-)}\sum_{i=1}^{3} j^{(+)}(i)\right] \qquad (6)$$

$$H_p = \sum_{i=1}^{3}\left[\frac{-\hbar^2}{2m_i}\nabla_i^2 + V_{Nilsson}(r_i)\right] \qquad (7)$$

$$H_j = \frac{1}{2\theta}\sum_{i=1}^{3}[(j^2(i) - j_3^2(i))] \qquad (8)$$

$$H_{PPC} = \frac{1}{2\theta}\sum_{i\angle k}^{3}[j^{(+)}(i)\, j^{(-)}(k) + j^{(-)}(i)\, j^{(+)}(k)] \qquad (9)$$

We have used the expression

$$\frac{1}{2\theta}\left[(\sum_{i=1}^{3} j(i))^2 - (\sum_{i=1}^{3} j_3(i))^2\right]$$
$$= \frac{1}{2\theta}\left[\sum_{i=1}^{3}\left(j^2(i) - j_3^2(i)\right)\right]$$
$$+ \frac{1}{2\theta}\sum_{i\angle k}^{3}[\mathrm{j}^{(+)}(i)\,\mathrm{j}^{(-)}(k) + \mathrm{j}^{(-)}(i)\,\mathrm{j}^{(+)}(k)] \qquad (10)$$

The diagonalization of the above Hamiltonian is performed in the basis of states

$$|IMKJ>= \sqrt{\frac{2I+1}{16\pi^2}}\,[D^{I}_{MK}(\alpha,\beta,\gamma)\,\psi_k + (-1)^{I-K} D^{I}_{M,-K}(\alpha,\beta,\gamma)\,\psi_{-k}] \qquad (11)$$

Here, $\psi_k$ represents the Nilsson single particle states ,with spin J which can be expanded into eigenstates of $J^2$

$$\psi_k = \sum_J C_{JK}|JK> \qquad (12)$$

M denote the projection of the total angular momentum I on the third axis in the laboratory frame where K denotes the projection of I on the third axis in the body – fixed frame. Since the total Hamiltonian is rotationally invariant, the quantum number M will be omitted.

If the three valence particles are confined in two Nilsson levels, namely with $\Omega_1 = \pm {}^1\!/_2$ and $\Omega_2 = \pm {}^3\!/_2$ , then the level structure of this system consists of two K bands ,$K = {}^1\!/_2$ *and* $K = {}^3\!/_2$ .

There are four wave functions

$$\psi_{1/2} = \frac{1}{\sqrt{6}}\{[\varphi_{3/2}(1)\varphi_{-3/2}(2)\varphi_{1/2}(3) + \varphi_{1/2}(1)\varphi_{3/2}(2)\varphi_{-3/2}(3)$$
$$+ \varphi_{-3/2}(1)\varphi_{1/2}(2)\varphi_{3/2}(3)]$$
$$- [\varphi_{3/2}(1)\varphi_{1/2}(2)\varphi_{-3/2}(3) + \varphi_{-3/2}(1)\varphi_{3/2}(2)\varphi_{1/2}(3)$$
$$+ \varphi_{1/2}(1)\varphi_{-3/2}(2)\varphi_{3/2}(3)]\} \qquad (13)$$

$$\psi_{-1/2} = \frac{1}{\sqrt{6}}\{[\varphi_{3/2}(1)\varphi_{-3/2}(2)\varphi_{-1/2}(3) + \varphi_{-1/2}(1)\varphi_{3/2}(2)\varphi_{-3/2}(3) + \varphi_{-3/2}(1)\varphi_{-1/2}(2)\varphi_{3/2}(3)] - [\varphi_{3/2}(1)\varphi_{-1/2}(2)\varphi_{-3/2}(3) + \varphi_{-3/2}(1)\varphi_{3/2}(2)\varphi_{-1/2}(3) + \varphi_{-1/2}(1)\varphi_{-3/2}(2)\varphi_{3/2}(3)]\} \quad (14)$$

$$\psi_{3/2} = \frac{1}{\sqrt{6}}\{[\varphi_{1/2}(1)\varphi_{-1/2}(2)\varphi_{3/2}(3) + \varphi_{3/2}(1)\varphi_{1/2}(2)\varphi_{-1/2}(3) + \varphi_{-1/2}(1)\varphi_{3/2}(2)\varphi_{1/2}(3)] - [\varphi_{1/2}(1)\varphi_{3/2}(2)\varphi_{-1/2}(3) + \varphi_{-1/2}(1)\varphi_{1/2}(2)\varphi_{3/2}(3) + \varphi_{3/2}(1)\varphi_{-1/2}(2)\varphi_{1/2}(3)]\} \quad (15)$$

$$\psi_{-3/2} = \frac{1}{\sqrt{6}}\{[\varphi_{1/2}(1)\varphi_{-1/2}(2)\varphi_{-3/2}(3) + \varphi_{-3/2}(1)\varphi_{1/2}(2)\varphi_{-1/2}(3) + \varphi_{-1/2}(1)\varphi_{-3/2}(2)\varphi_{1/2}(3)] - [\varphi_{1/2}(1)\varphi_{-3/2}(2)\varphi_{-1/2}(3) + \varphi_{-1/2}(1)\varphi_{1/2}(2)\varphi_{-3/2}(3) + \varphi_{-3/2}(1)\varphi_{-1/2}(2)\varphi_{1/2}(3)]\} \quad (16)$$

The bases functions for the total Hamiltonian have the form

$$|1\rangle = \left|\frac{1}{2}\right\rangle = \sqrt{\frac{2I+1}{16\pi^2}}\left|D^I_{M,1/2}(\alpha\beta\gamma)\psi_{1/2} + (-1)^{I+j}D^I_{M,-1/2}(\alpha\beta\gamma)\psi_{-1/2}\right| \quad (17)$$

$$|2\rangle = \left|\frac{3}{2}\right\rangle = \sqrt{\frac{2I+1}{16\pi^2}}\left|D^I_{M,3/2}(\alpha\beta\gamma)\psi_{3/2} + (-1)^{I+j}D^I_{M,-3/2}(\alpha\beta\gamma)\psi_{-3/2}\right| \quad (18)$$

Diagonalize of the total Hamiltonian between the two bases states with

$K = {}^{1}/_{2}$ *and* $K = {}^{3}/_{2}$, yield

$$\langle 1|\hat{H}|\,1\rangle = \frac{1}{2\theta}[I(I+1)-\frac{1}{4}] + \frac{C}{2}\,(\theta_I-\theta)^2 - \frac{1}{2\theta}(-1)^{I+j} + \left(I+\frac{1}{2}\right)\left\langle\varphi_{1/2}\middle|j^{(+)}\middle|\varphi_{-1/2}\right\rangle + E_p + [2\left\langle\varphi_{3/2}\middle|j^2-j_3^2\middle|\varphi_{3/2}\right\rangle + \left\langle\varphi_{1/2}\middle|j^2-j_3^2\middle|\varphi_{1/2}\right\rangle - \frac{1}{2\theta}[\left\langle\varphi_{3/2}\middle|j^{(+)}\middle|\varphi_{1/2}\right\rangle]^2 \quad (19)$$

$$\langle 1\,|\hat{H}|\,2\rangle = \langle 2\,|\hat{H}|\,1\rangle = \frac{1}{2\theta}\sqrt{(I-\frac{1}{2})(I+\frac{3}{2})}\left\langle\varphi_{3/2}\middle|j^{(+)}{}_{(i)}\middle|\varphi_{1/2}\right\rangle \quad (20)$$

$$\langle 2\,|\hat{H}|\,2\rangle = \frac{1}{2\theta}[I(I+1)-\frac{9}{4}] + \frac{C}{2}\,(\theta_I-\theta)^2 + E_p + [2\left\langle\varphi_{1/2}\middle|j^2-j_3^2\middle|\varphi_{1/2}\right\rangle + \left\langle\varphi_{3/2}\middle|j^2-j_3^2\middle|\varphi_{3/2}\right\rangle] - \frac{1}{2\theta}\{\left[\left\langle\varphi_{3/2}\middle|j^{(+)}\middle|\varphi_{1/2}\right\rangle\right]^2 + \left[\left\langle\varphi_{1/2}\middle|j^{(+)}\middle|\varphi_{-1/2}\right\rangle\right]^2\right\} \quad (21)$$

The matrix elements of the single-particle operators $j^2$, $j_3^2$ and $j^{(\pm)}$ are calculated by using the deformed Nilsson wave functions.

### 3-Kinematic and Dynamic Moments of Inertia

Two types of moments of inertia are usually discussed :The Kinematic(or first ) moment of inertia

$$\frac{J^{(1)}}{\hbar^2} = \left[\frac{1}{\hat{I}}\frac{dE_{rot}}{d\hat{I}}\right]^{-1} \quad , \quad \hat{I} = \sqrt{I(I+1)}$$

and the dynamic ( or second) moment of inertia defined as

$$\frac{J^{(2)}}{\hbar^2} = \left[\frac{d^2E_{rot}}{d\hat{I}^2}\right]^{-1}$$

These two moments of inertia are obviously dependent

$$J^{(2)} = (\frac{d}{dI}\frac{dE_{rot}}{dI})^{-1} = (\frac{d\omega}{dI})^{-1} = \frac{dI}{d\omega} = \frac{d}{d\omega}\left(\omega J^{(1)}\right) = J^{(1)} + \omega\frac{dJ^{(1)}}{d\omega}$$

In the case of a rigid- rotor both , the kinematic $J^{(1)}$ and dynamic $J^{(2)}$ moments of inertia coincide.

Using the intraband $E_2$ transition energies the two moments of inertia and the rotational frequency are written as

$$\frac{J^{(1)}}{\hbar^2} = \frac{2I-1}{E_\gamma\ (I \to I-2)}$$

$$\frac{J^{(2)}}{\hbar^2} = \frac{4}{E_\gamma(I+2 \to I) - E_\gamma\ (I \to I-2)}$$

$$\hbar\omega = \frac{1}{4}\left[E_\gamma(I+2 \to I) + E_\gamma\ (I \to I-2)\right]$$

It is seen that, while the extracted $J^{(1)}$ depends on the spin I proposition, $J^{(2)}$ does not.

**4-THE ΔI = 1 ENERGY STAGGERING**

A plot of $E_\gamma(I) = E(I) - E(I-1)$ versus I is the most simple way to identify the signature splitting of two signatures , the effect shows up as a reversal of the phase of the staggering . Also in previous papers[44-50] we have considered a staggering function depends only on the quadrupole transitions with each band of the partners.

To investigate the ΔI = 1 energy staggering in signature partner pairs of odd –A SD bands ,was propose in this paper ,two staggering functions: the first one is the index $Y(I)$ which depends on the dipole transition energies $E_{\gamma 1}$linking the two signature partners and the quadruple transition energies $E_{\gamma 2}$ within each band , such that

$$Y(I) = \left(\frac{2I-1}{I}\right)\left(\frac{E(I) - E(I-1)}{E(I) - E(I-2)}\right) - 1$$

$$= \left(\frac{2I-1}{I}\right)\left(\frac{E_{\gamma 1}(I)}{E_{\gamma 2}(I)}\right) - 1$$

where

$$E_{\gamma 1}(I) = E(I) - E(I-1)$$

$$E_{\gamma 2}(I) = E(I) - E(I-2)$$

This staggering index $Y(I)$ vanishes for a strongly coupled rotational band.

The second staggering function is the index $S(I)$ which depends on the dipole transition energies linking the two signature partners.

$$S(I) = \frac{1}{2}[E_{\gamma 1}(I+1) - 2E_{\gamma 1}(I) + E_{\gamma 1}(I-1)]$$

An anomalous signature splitting can occur when plotting $S(I)$ as a function of the rotational frequency

$$\hbar\omega(I \to I-1) = \frac{1}{4}[\hbar\omega(I+2 \to I) + \hbar\omega(I \to I-2) + \hbar\omega(I+1 \to I-1) + \hbar\omega(I-1 \to I-3)]$$

**5- RESULTS and DISCUSSION**

Since the amount of signature splitting and alignment is dependent on the $\Omega = 1/2$ component mixed into the particle wavefunction , the fact that a consistent picture exists for $j_{15/2}$ intruder pairs at N =( 110-113) is remarkable and indicates that the relative excitation energies of the $\Omega = 3/2$ orbit in the $j_{15/2}$ subshell is correct at large deformation .Therefore , in our suggested PRM , we considered that the three extra core particles occupy only two Nilsson levels with$\Omega = |1/2|$ and $\Omega = |3/2|$. The total Hamiltonian is diagonalzid between the two basis functions and the results of the diagonalzation are the exact excitation energies.

We have performed calculations for single particle energy levels using the deformed model with the optimized $\kappa,\mu$ Nilsson parameters and the quadrupole deformation parameter $\beta_2$ listed in Table(1) which provide a good description of the single- particle levels and the shell structure for our selected odd-mass nuclei. The correct bandhead spins and bandhead excitation energies and the two parameters $\theta_0$, C of the VMI model for all SD bands choosen are given in Table(2).

The transition energies $E_\gamma(I)$are used to calculated the kinematic $J^{(1)}$ and dynamic $J^{(2)}$ moments of inertia and the rotational frequency $\hbar\omega$ of the studied ten SD bands . The variation of the calculated kinematic $J^{(1)}$ ( open circles ) and the dynamic $J^{(2)}$ ( solid curves ) moments of inertia and the experimental $J^{(2)}$ ( closed circles with error bars ) as a function of rotational frequency $\hbar\omega$ are shown in Figures (1 , 2). We see that smooth increase of $J^{(2)}$ with $\hbar\omega$ is reproduced well and $J^{(1)}$ is found to be smaller than that $J^{(2)}$ for all values of $\hbar\omega$ and the values of $J^{(1)}$ and $J^{(2)}$ approaches each other at the bandhead spin $I_0$ .

To investigate the $\Delta I = 1$ energy staggering in our five pairs of signature partners $^{191}$Hg (SD2,SD3) , $^{193}$Hg (SD1,SD2) , $^{193}$Hg (SD3,SD4) , $^{191}$Tl (SD1,SD2) and $^{193}$Tl (SD1,SD2), the staggering indices Y(I) and S(I) are calculated and their values as a function of spin I or rotational frequency $\hbar\omega$ for each signature partner are listed in Tables (3,4) and plotted in Figures (3 , 4,5,6). All the signature partners show large amplitude staggering.

## 6- CONCLUSION

The Nilsson plus particle rotor model (PRM) has been used to fit the $\gamma$ - transition energies of the SD bands . We have considered the odd-A nucleus consists of axially symmetric core with variable moment of inertia and three valence particles occupy two Nilsson levels with projections 1/2 and 3/ 2.

The selected SD bands are the five pairs of signature partners namely $^{191}$Hg (SD2,SD3) , $^{193}$Hg (SD1,SD2), $^{193}$Hg (SD3,SD4), $^{191}$Tl (SD1,SD2) and $^{193}$Tl (SD1,SD2).The optimized model parameters are extracted and the spins, excitation energies , rotational frequencies , kinematic and dynamic moments of inertia are calculated and analyzed and compared with the experimental data . The feature of $\Delta$ I=1 energy staggering in these SD signature partners are outlined by suggested two staggering indices depend on the dipole transitions linking the two signatures and the quadrupole transitions within each band.

**Table (1): The single- particle Nilsson parameters $\kappa$ , $\mu$ and the deformation parameters $\beta_2$ in each individual nucleus for the selected Hg and Tl nuclei .**

| Nucleus | $\beta_2$ | $\kappa$ | $\mu$ |
|---|---|---|---|
| $^{191}$Hg | 0.42 | 0.0636 | 0.3883 |
| $^{193}$Hg | 0.44 | 0.0636 | 0.3858 |
| $^{191}$Tl | 0.50 | 0.0636 | 0.3826 |
| $^{193}$Tl | 0.51 | 0.0616 | 0.6183 |

**Table (2): Suggested bandhead spin proposition $I_0$ and excitation energy $E_{bh}$ and the adopted $J_0$ and C of VMI, used in the calculations for five pairs of signature partners SD bands.**

| signature partner SD bands | $I_0$ ($\hbar$) | $E_{bh}$ (KeV) | $J_0$ ($\hbar^2 MeV^{-1}$) | $C\times10^{-3}$ $(MeV)^3$ | $J^{(1)}_{bh}$ ($\hbar^2 MeV^{-1}$) |
|---|---|---|---|---|---|
| $^{191}$Hg(SD2) | 10.5 | 638.475 | 94.743 | 9.7755 | 95.186 |
| (SD3) | 11.5 | 758.152 | 93.849 | 5.9598 | 95.262 |
| $^{193}$Hg(SD1) | 9.5 | 548.497 | 98.755 | 1.8319 | 93.649 |
| (SD2) | 10.5 | 645.213 | 92.934 | 5.5074 | 94.481 |
| $^{193}$Hg(SD3) | 9.5 | 533.845 | 94.648 | 5.4214 | 94.181 |
| (SD4) | 10.5 | 646.129 | 92.667 | 4.5820 | 94.481 |
| $^{191}$Tl (SD1) | 11.5 | 771.457 | 92.700 | 8.0970 | 93.811 |
| (SD2) | 12.5 | 910.156 | 92.101 | 8.3098 | 93.518 |
| $^{193}$Tl (SD1) | 8.5 | 419.427 | 96.000 | 8.4000 | 96.655 |
| (SD2) | 9.5 | 517.485 | 96.100 | 9.7000 | 96.784 |

**Table (3): The calculated Δ I= 1 staggering index Y(I) for our selected five signature partner pairs in Hg and Tl odd-A superdeformed nuclei and comparison with the experimental data and comparison with experimental data .**

| $^{191}$Hg(SD2, SD3) | | | $^{193}$Hg(SD1, SD2) | | | $^{193}$Hg(SD3, SD4) | | |
|---|---|---|---|---|---|---|---|---|
| I(ħ) | Y(I)(KeV) Exp | Y(I)(KeV) Cal | I(ħ) | Y(I)(KeV) Exp | Y(I)(KeV) Cal | I (ħ) | Y(I)(KeV) Exp | Y(I)(KeV) Cal |
| 12.5 | 0.0096 | 0.014 | 11.5 | 0.1196 | 0.1254 | 11.5 | -0.0068 | -0.0065 |
| 13.5 | -0.0138 | -0.018 | 12.5 | -0.1116 | -0.1246 | 12.5 | 0.0037 | 0.0030 |
| 14.5 | 0.0121 | 0.016 | 13.5 | 0.1005 | 0.1157 | 13.5 | -0.0033 | -0.0045 |
| 15.5 | -0.0129 | -0.016 | 14.5 | -0.1012 | -0.1113 | 14.5 | -0.0024 | 0.0012 |
| 16.5 | 0.0097 | 0.013 | 15.5 | 0.0903 | 0.1028 | 15.5 | 0.0009 | -0.0034 |
| 17.5 | -0.0128 | -0.016 | 16.5 | -0.0803 | -0.0903 | 16.5 | -0.004 | 0.0002 |
| 18.5 | 0.0108 | 0.014 | 17.5 | 0.0697 | 0.0833 | 17.5 | 0.0018 | -0.0031 |
| 19.5 | -0.0150 | -0.018 | 18.5 | -0.0651 | -0.0740 | 18.5 | -0.0050 | 0.0 |
| 20.5 | 0.0136 | 0.016 | 19.5 | 0.0540 | 0.0584 | 19.5 | 0.0001 | -0.0049 |
| 21.5 | -0.0190 | -0.022 | 20.5 | -0.0500 | -0.0513 | 20.5 | -0.0043 | 0.0003 |
| 22.5 | 0.0184 | 0.021 | 21.5 | 0.0376 | 0.0324 | 21.5 | 0.0005 | -0.0043 |
| 23.5 | -0.0253 | -0.028 | 22.5 | -0.0323 | -0.0185 | 22.5 | -0.0038 | 0.0011 |
| 24.5 | 0.0256 | 0.028 | 23.5 | 0.0165 | -0.0035 | 23.5 | 0.0003 | -0.0056 |
| 25.5 | -0.0335 | -0.036 | 24.5 | -0.0085 | 0.0172 | 24.5 | -0.0038 | 0.0023 |
| 27.5 | -0.0435 | -0.046 | 26.5 | 0.0266 | 0.0577 | 26.5 | -0.0019 | 0.0110 |
| 28.5 | 0.0451 | 0.047 | 27.5 | -0.0572 | -0.0867 | 27.5 | -0.0045 | -0.0232 |
| 29.5 | -0.0553 | -0.057 | 28.5 | 0.0749 | 0.1022 | 28.5 | 0.0015 | 0.0192 |
| 30.5 | 0.0571 | 0.089 | 29.5 | -0.1122 | -0.1343 | 29.5 | -0.0066 | -0.0240 |
| 31.5 | -0.0681 | -0.070 | 30.5 | 0.1332 | 0.1476 | 30.5 | 0.0035 | 0.0198 |
| 32.5 | 0.0702 | 0.072 | 31.5 | -0.1750 | -0.1842 | 31.5 | -0.0088 | -0.0246 |
| 33.5 | -0.0830 | -0.085 | 32.5 | 0.1948 | 0.1985 | 32.5 | 0.0052 | 0.0203 |
| 34.5 | 0.0860 | 0.087 | 33.5 | -0.2371 | -0.2349 | 33.5 | -0.0113 | -0.0251 |
| 35.5 | -0.0987 | -0.100 | 34.5 | 0.2528 | 0.2475 | 34.5 | 0.0079 | 0.0206 |
| 36.5 | 0.1241 | 0.103 | 35.5 | -0.2930 | -0.2848 | 35.5 | -0.0125 | -0.0252 |
| 37.5 | -0.1153 | -0.171 | 36.5 | 0.3045 | 0.2951 | 36.5 | 0.0079 | 0.0205 |
| 38.5 | 0.1182 | 0.120 | 37.5 | -0.3422 | -0.3320 | 37.5 | -0.0125 | -0.0249 |
| 39.5 | -0.1329 | -0.134 | 38.5 | 0.3497 | 0.3398 | 38.5 | 0.0076 | 0.0200 |
| 40.5 | 0.1365 | 0.138 | 39.5 | -0.3835 | -0.3750 | 39.5 | -0.0107 | -0.0241 |
| 41.5 | -0.1540 | -0.153 | 40.5 | 0.3874 | 0.380 | 40.5 | 0.0045 | 0.0192 |
| 42.5 | 0.1570 | 0.156 | 41.5 | -0.4181 | -0.41241 | 41.5 | -0.0099 | -0.0232 |
| 43.5 | -0.1725 | -0.174 | 42.5 | 0.4196 | 0.4148 | 42.5 | 0.00635 | 0.0183 |
| | | | 43.5 | -0.4474 | -0.4433 | 43.5 | -0.0109 | -0.0223 |
| | | | 44.5 | 0.4469 | 0.4432 | 44.5 | 0.0069 | 0.0176 |
| | | | 45.5 | -0.4712 | -0.4675 | 45.5 | -0.0117 | -0.0220 |
| | | | 47.5 | -0.4789 | -0.4746 | 46.5 | 0.0080 | 0.0179 |

**Table (3): Continued**

| $^{191}$T1(SD1, SD2) | | | $^{193}$T1(SD1, SD2) | | |
|---|---|---|---|---|---|
| I(ħ) | Y(I)(KeV) Exp | Y(I)(KeV) Cal | I(ħ) | Y(I)(KeV) Exp | Y(I)(KeV) Cal |
| 13.5 | -0.0401 | -0.0378 | 10.5 | 0.0007 | 0.0021 |
| 14.5 | 0.0329 | 0.0380 | 11.5 | -0.0004 | -0.0031 |
| 15.5 | -0.0301 | -0.0425 | 12.5 | -0.0020 | 0.0013 |
| 16.5 | 0.0237 | 0.0420 | 13.5 | 0.0018 | -0.0023 |
| 17.5 | -0.0204 | -0.0465 | 14.5 | -0.0043 | 0.0 |
| 18.5 | 0.0136 | 0.0454 | 15.5 | 0.0039 | -0.0008 |
| 19.5 | -0.0129 | -0.0497 | 16.5 | -0.0075 | 0.0221 |
| 20.5 | 0.0057 | 0.0479 | 17.5 | 0.0074 | 0.0015 |
| 21.5 | -0.0043 | -0.522 | 18.5 | -0.0124 | -0.0053 |
| 22.5 | -0.0031 | 0.0496 | 19.5 | 0.0124 | 0.0048 |
| 23.5 | 0.0037 | -0.0536 | 20.5 | -0.0167 | -0.0094 |
| 24.5 | -0/.0128 | 0.0502 | 21.5 | 0.0155 | 0.0093 |
| 25.5 | 0.0145 | -0.0540 | 22.5 | -0.0182 | -0.0148 |
| 26.5 | -0.0240 | 0.0497 | 23.5 | 0.0213 | 0.0150 |
| 27.5 | 0.0256 | -0.0530 | 24.5 | -0.0290 | -0.0215 |
| 28.5 | -0.0347 | 0.0478 | 25.5 | 0.0305 | 0.0221 |
| 29.5 | 0.0354 | -0.0509 | 26.5 | -0.0390 | -0.0297 |
| 30.5 | -0.0470 | 0.0447 | 27.5 | 0.0402 | 0.0307 |
| 31.5 | 0.0480 | -0.0474 | 28.5 | -0.0494 | -0.0395 |
| 32.5 | -0.0601 | 0.0401 | 29.5 | 0.0511 | 0.0410 |
| 33.5 | 0.0626 | -0.0422 | 30.5 | -0.0610 | -0.0512 |
| 34.5 | -0.0768 | 0.0338 | 31.5 | 0.0631 | 0.0532 |
| 35.5 | 0.0802 | -0.0354 | 32.5 | -0.0747 | -0.0649 |
| 36.5 | -0.0961 | 0.0256 | 33.5 | 0.0782 | 0.0675 |
| 37.5 | 0.0986 | -0.0265 | 34.5 | -0.0915 | -0.0807 |
| 38.5 | -0.1144 | 0.0153 | 35.5 | 0.0966 | 0.0839 |
| | | | 36.5 | -0.1126 | -0.0990 |
| | | | 37.5 | 0.1193 | 0.1028 |
| | | | 38.5 | -0.1371 | -0.1200 |
| | | | 39.5 | 0.1448 | 0.1244 |
| | | | 40.5 | -0.1640 | -0.1439 |
| | | | 41.5 | 0.1724 | 0.1488 |
| | | | 42.5 | -0.1940 | -0.1709 |

**Table(4): The same as in Table(3) but for the staggering index S(I) as function of rotational frequency ħω.**

| $^{191}$Hg(SD2, SD3) | | | $^{193}$Hg(SD1, SD2) | | | $^{193}$Hg(SD3, SD4) | | |
|---|---|---|---|---|---|---|---|---|
| ħω (MeV) | S(I) (KeV) Exp | Cal | ħω (MeV) | S(I) (KeV) Exp | Cal | ħω (MeV) | S(I) (KeV) Exp | Cal |
| 0.141 | 3.796 | 1.9955 | 0.132 | 29.968 | 33.0355 | 0.132 | -0.968 | -1.0655 |
| 0.151 | -3.946 | -2.6225 | 0.142 | -29.368 | -33.9005 | 0.142 | 0.068 | 0.8185 |
| 0.161 | 3.746 | 4.002 | 0.152 | 29.668 | 34.0205 | 0.152 | 0.532 | -0.7675 |
| 0.171 | -4.021 | -5.971 | 0.162 | -28.918 | -33.717 | 0.162 | -0.982 | 0.5190 |
| 0.180 | 4.396 | 8.2405 | 0.172 | 26.918 | 32.039 | 0.172 | 1.132 | -0.6395 |
| 0.190 | -5.121 | -10.766 | 0.181 | -25.218 | -29.3395 | 0.182 | -1.332 | 0.5600 |
| 0.200 | 5.896 | 13.2375 | 0.191 | 23.368 | 25.889 | 0.192 | 1.182 | -0.8705 |
| 0.210 | -7.096 | -15.7535 | 0.200 | -21.468 | -22.302 | 0.201 | -1.182 | 1.049 |
| 0.219 | 8.446 | 17.9855 | 0.210 | 18.818 | 17.624 | 0.211 | 1.032 | -1.2015 |
| 0.229 | -10.346 | -20.186 | 0.219 | -15.718 | -11.5455 | 0.220 | -1.032 | 1.2165 |
| 0.239 | 12.446 | 22.016 | 0.228 | 11.318 | 3.559 | 0.230 | 0.882 | -1.6405 |
| 0.248 | -15.046 | -23.8865 | 0.237 | -6.018 | 5.2155 | 0.239 | -0.982 | 1.918 |
| 0.257 | 17.796 | 25.448 | 0.246 | -1.382 | -15.249 | 0.249 | 0.682 | -2.555 |
| 0.266 | -21.196 | -27.252 | 0.254 | 10.582 | 26.3585 | 0.258 | -0.282 | 4.834 |
| 0.275 | 24.896 | 28.948 | 0.263 | -22.682 | -38.9545 | 0.267 | -0.768 | -9.4575 |
| 0.284 | 29.146 | -31.193 | 0.271 | 36.8 82 | 52.617 | 0.275 | 1.668 | 11.906 |
| 0.293 | 33.546 | 33.634 | 0.280 | -53.432 | -67.672 | 0.284 | -2.418 | -12.5745 |
| 0.302 | -38.496 | -36.970 | 0.288 | 72. 332 | 83.7055 | 0.292 | 3.018 | 13.049 |
| 0.310 | 43.671 | 40.853 | 0.297 | -92.982 | -100.967 | o.301 | -3.868 | -13.7105 |
| 0.319 | -49.721 | -45.933 | 0.305 | 114.832 | 119.056 | 0.309 | 4.418 | 14.1585 |
| 0.327 | 56.196 | 51.8655 | 0.313 | -137.332 | -138.134 | 0.318 | -5.418 | -14.758 |
| 0.335 | -62.996 | -59.121 | 0.321 | 159.982 | 157.82 | 0.326 | 6.368 | 15.128 |
| 0.343 | 73.946 | 67.3625 | 0.329 | -182.532 | -178.3345 | 0.334 | -7.018 | -15.615 |
| 0.351 | -85.546 | -76.7125 | 0.337 | 204.732 | 198.8895 | 0.342 | 7.118 | 15.8615 |
| 0.357 | 89.346 | 86.8855 | 0.345 | -226.733 | -219.919 | 0.350 | -7.368 | -16.1955 |
| 0.367 | -93.796 | -97.1035 | 0.353 | 248.082 | 240.9535 | 0.358 | 7.318 | 16.291 |
| 0.376 | 102.746 | 107.6785 | 0.361 | -268.782 | -261.945 | 0.366 | -6.868 | -16.463 |
| | | | 0.369 | 288.582 | 282.603 | 0.374 | 5.768 | 16.421 |
| | | | 0.377 | -307.932 | -302.854 | 0.382 | -5.668 | -16.471 |
| | | | 0.385 | 326.682 | 322.4465 | 0.389 | 6.418 | 16.3615 |
| | | | 0.392 | -344.932 | -341.331 | 0.397 | -7.018 | -16.3995 |
| | | | 0.400 | 362.532 | 355.2975 | 0.404 | 7.318 | 16.375 |
| | | | 0.408 | -379.482 | -376.3725 | 0.412 | -7.868 | -16.613 |
| | | | 0.416 | 395.482 | 392.391 | | | |

**Table (4): Continued**

| $^{191}$Tl(SD1, SD2) | | | $^{193}$Tl(SD1, SD2) | | |
|---|---|---|---|---|---|
| ħω (MeV) | S(I) (KeV) | | ħω (MeV) | S(I) (KeV) | |
| | Exp | Cal | | Exp | Cal |
| 0.154 | -9.998 | -12.94 | 0.118 | -0.216 | 0.5415 |
| 0.164 | 9.048 | 14.403 | 0.128 | 0.516 | -0.509 |
| 0.174 | -7.898 | -16.032 | 0.138 | -0.916 | 0.3095 |
| 0.185 | 6.398 | 17.5065 | 0.148 | 1.266 | -0.132 |
| 0.195 | -5.298 | -19.134 | 0.158 | -1.915 | -0.2595 |
| 0.205 | 3.698 | 20.5565 | 0.168 | 2.613 | 0.648 |
| 0.214 | -2.198 | -22.117 | 0.178 | -3.713 | -1.3025 |
| 0.224 | 0.198 | 23.4075 | 0.188 | 4.815 | 1.976 |
| 0.234 | 1.652 | -24.807 | 0.198 | -5.966 | -2.971 |
| 0.243 | -4.202 | 25.877 | 0.207 | 6.866 | 4.012 |
| 0.253 | 7.052 | -27.033 | 0.217 | -7.866 | -5.4355 |
| 0.262 | -10.352 | 27.762 | 0.226 | 9.216 | 6.937 |
| 0.271 | 13.702 | -28.515 | 0.236 | -11.916 | -8.887 |
| 0.281 | -17.252 | 28.833 | 0.245 | 14.916 | 10.952 |
| 0.289 | 20.602 | -29.204 | 0.254 | -18.116 | -13.535 |
| 0.298 | -25.002 | 29.035 | 0.263 | 21.316 | 16.273 |
| 0.307 | 29.552 | -28.849 | 0.272 | -24.966 | -19.6035 |
| 0.316 | -34.602 | 28.044 | 0.281 | 28.816 | 23.135 |
| 0.324 | 40.252 | -27.1805 | 0.290 | -33.166 | -27.3385 |
| 0.332 | -46.902 | 25.616 | 0.298 | 37.766 | 31.7935 |
| 0.340 | 54.052 | -23.9455 | 0.307 | -43.166 | -37.005 |
| 0.348 | -62.152 | 21.4865 | 0.315 | 49.166 | 42.5235 |
| 0.356 | 70.052 | -18.8715 | 0.325 | -56.016 | -48.8855 |
| | | | 0.332 | 63.666 | 55.6125 |
| | | | 0.340 | -72.516 | -63.2785 |
| | | | 0.348 | 82.366 | 71.375 |
| | | | 0.355 | -93.166 | -80.5065 |
| | | | 0.363 | 104.816 | 90.1365 |
| | | | 0.371 | -117.316 | -101.9045 |
| | | | 0.378 | 130.716 | 112.2455 |

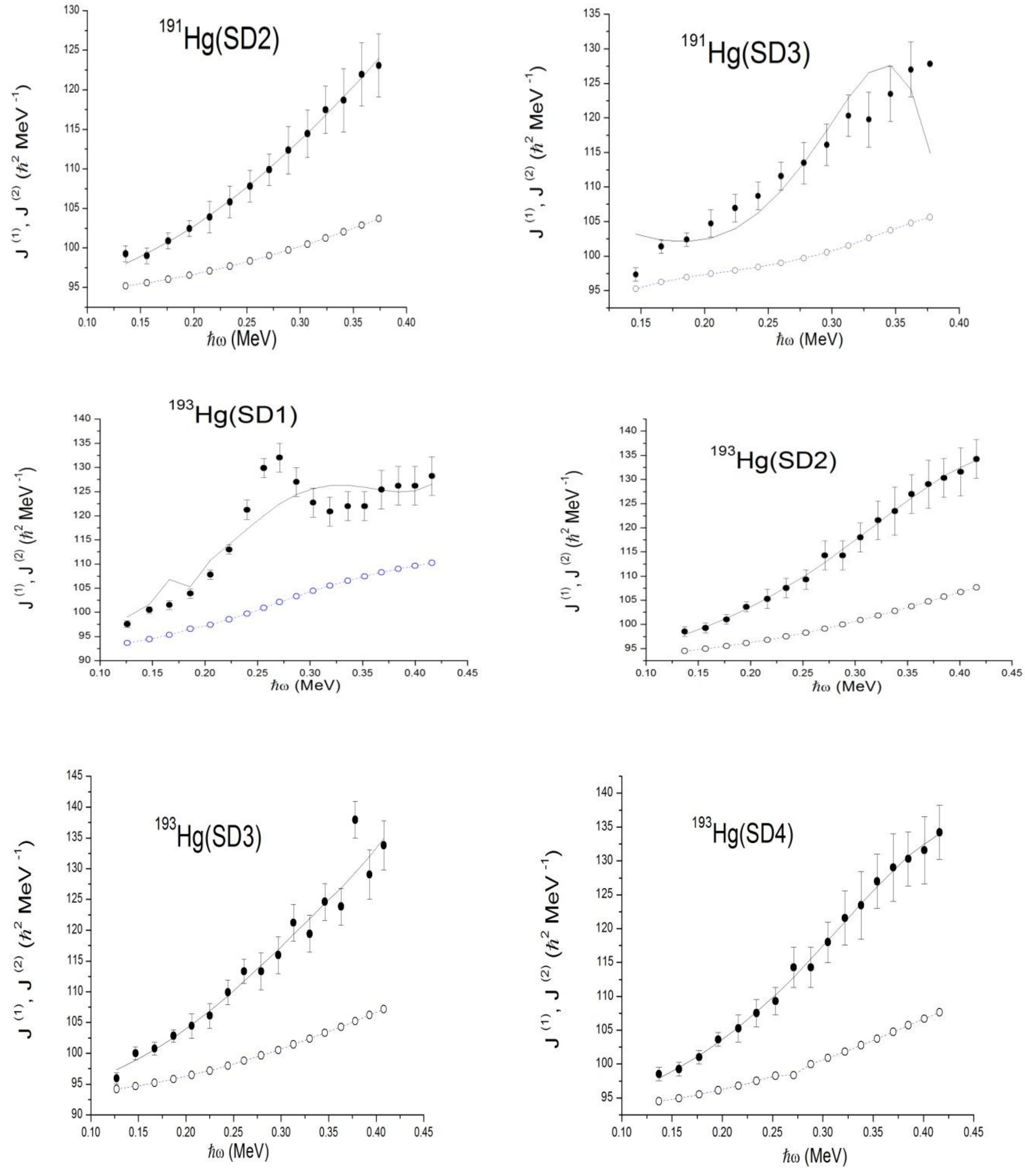


**Figure (1) :The calculated values of kinematic moment of inertia $J^{(1)}$ ( open circles) and the dynamic moment of inertia $J^{(2)}$ ( solid curve ) as a function of rotational frequency ħω for the three SD signature partner pairs $^{191}$Hg (SD2,SD3), $^{193}$Hg (SD1,SD2) , $^{193}$Hg (SD3,SD4) and comparison with the experimental data for $J^{(2)}$( closed circles with error bars). The experimental transition energies are taken from Ref. [3]. In computation $J^{(1)}$ we used the bandhead spins listed in Table(1).**

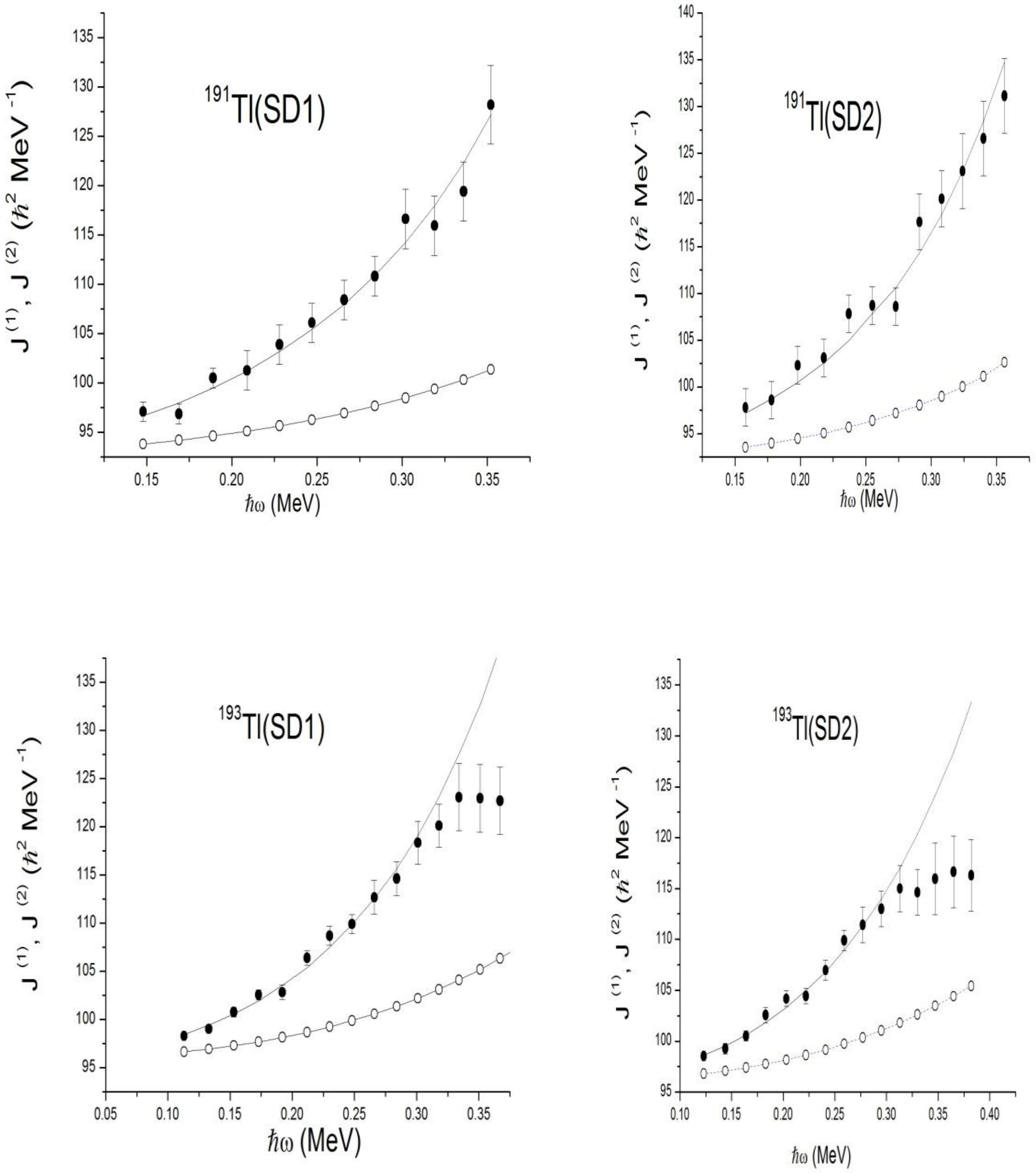


**Figure (2): The same as Figure (1) but for the signature partners $^{191}$Tl (SD1,SD2) and $^{193}$Tl (SD1,SD2).**

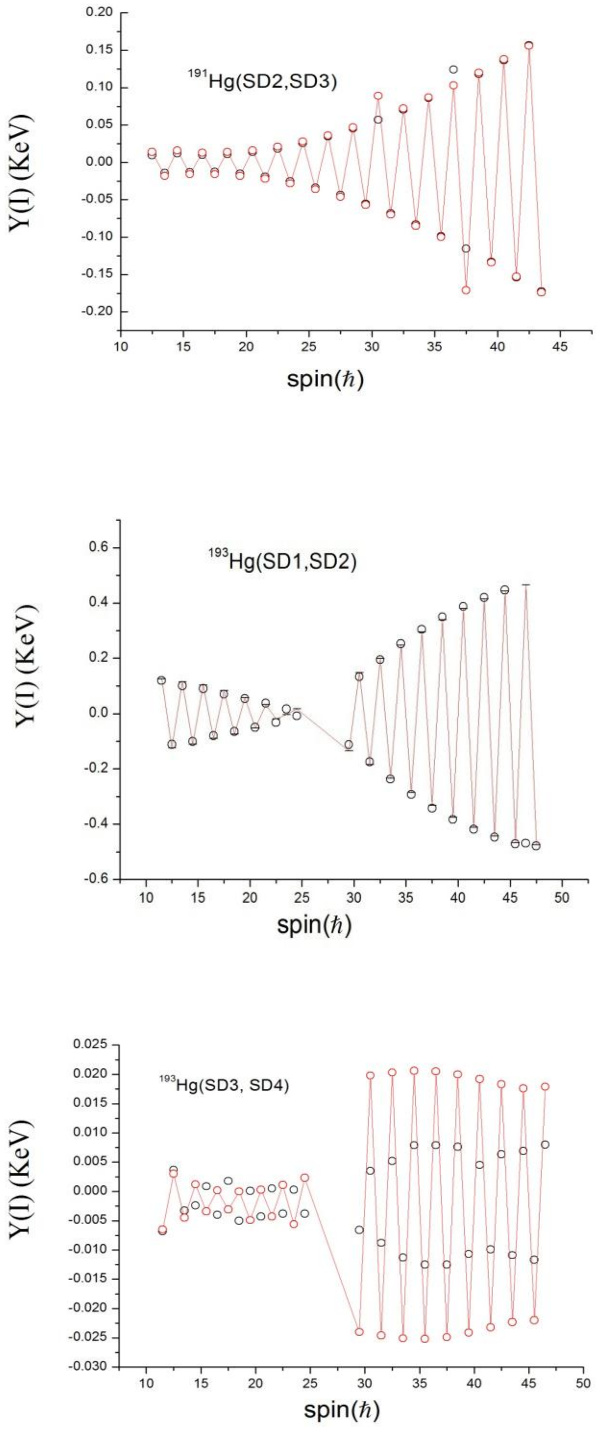


**Figure (3): The calculated ΔI=1 staggering index Y(I) (solid curve) as a function of nuclear spin I for the signature partner pairs $^{191}$Hg(SD2,SD3), $^{193}$Hg(SD2,SD2) and, $^{193}$Hg(SD3,SD4). The experimental values are represented by dots. Note that the scale is different in all plots of this figure. The experimental transition energies are taken from Ref. [3].**

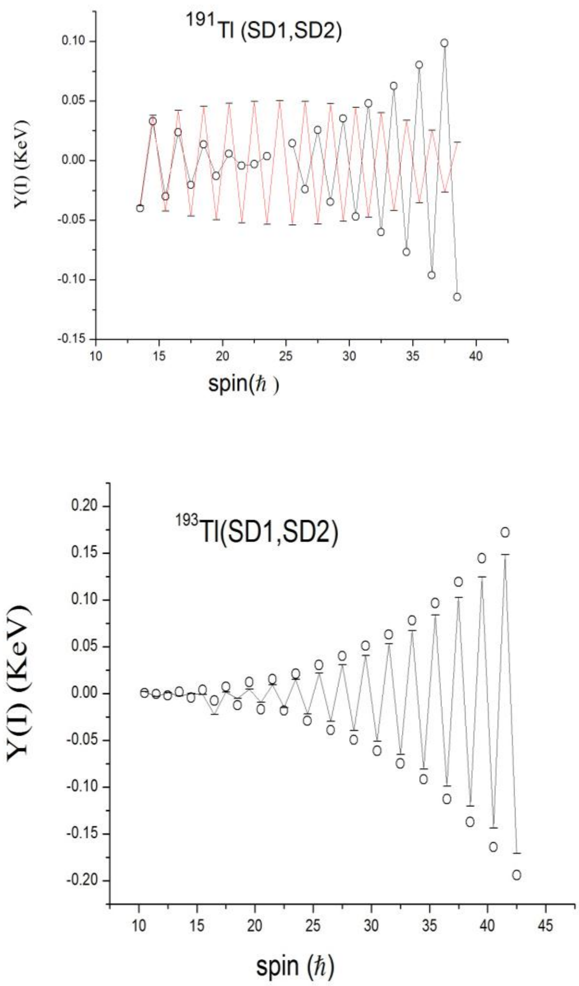


**Figure (4): The same as Figure (3) but for the signature partner pairs $^{191}$Tl(SD1, SD2) and $^{193}$Tl(SD1, SD2).**

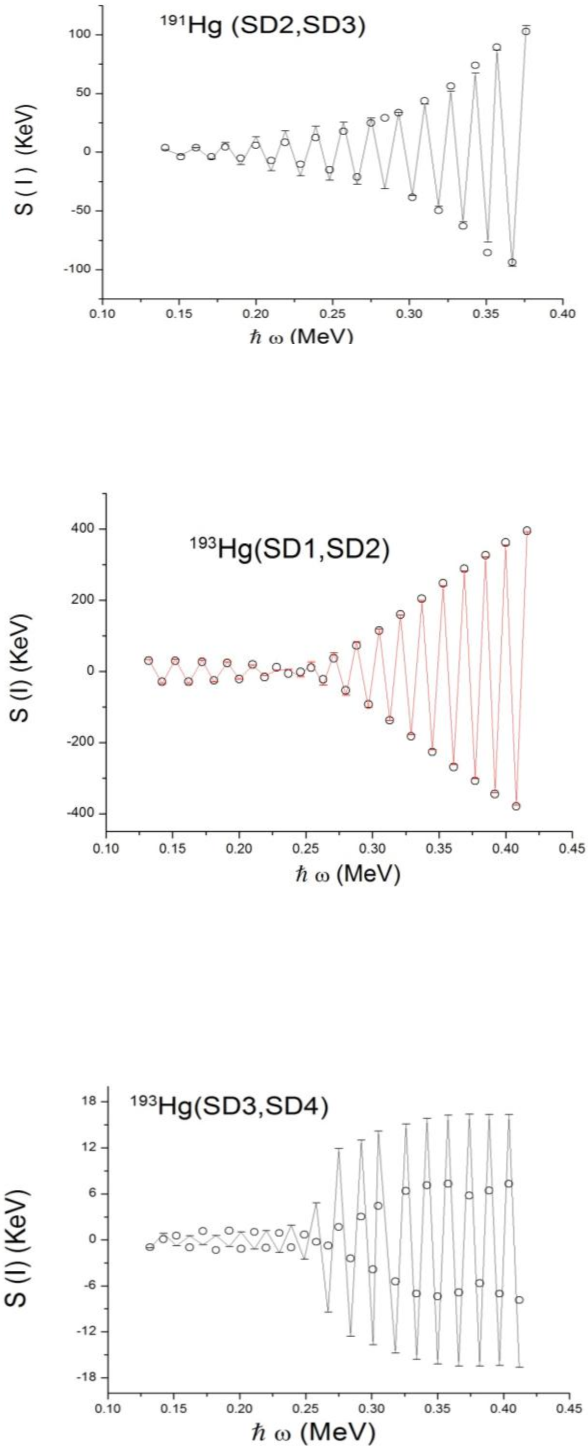


**Figure (5): The same as in Figure (1) but for the staggering index S(I) as a function of rotational frequency ħω (MeV)**

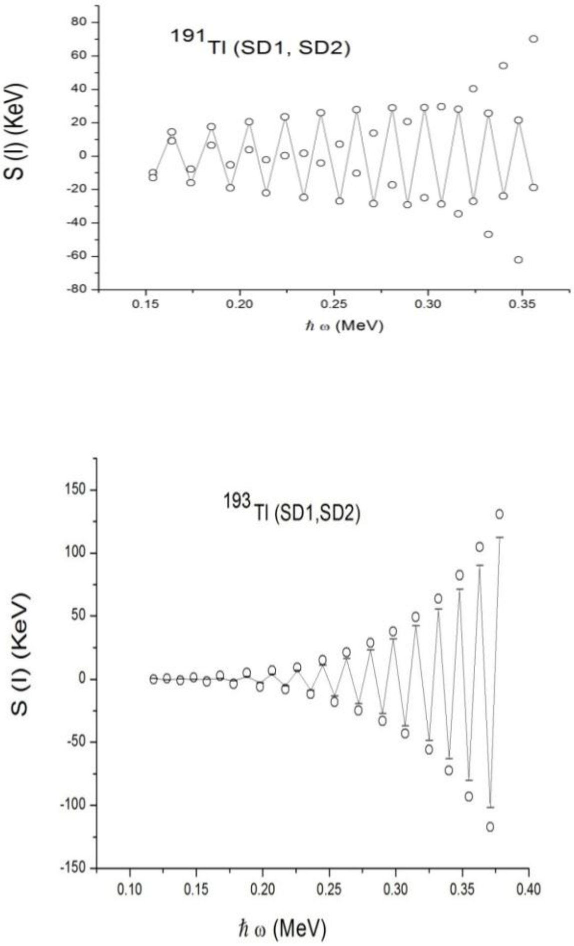


**Figure (6): The same as in Figure (2) but for the staggering index S(I) as a function of rotational frequency ħω (MeV).**

**7- REFERENCES**

[1] P.J. Twin et al, Phys. Rev. Lett. 57(1986) 811.
[2] B. Singh, R. Zymvina and R.B. Firestone, Nuclear Data Sheets 97 (2002)241.
[3] National Nuclear Data Center NNDC, Brookhaven National Laboratory [Cited on July 2012] http. //www.nndc.bnl.gov/chart/.
[4] M.A.Riley ,et al, Nucl. Phys. A512 (1990)178
[5] M.W.Drigert, et al, Nucl. Phys. A530 (1991) 452
[6] P.J. Nolan and P.J. Twin, Ann. Rev. Nucl. Part. Sci. 38 (1988)533
[7] R. V. F. Janssens and T.L. Khoo, Ann. Rev. Nucl. Part. Sci., 41( 1991)321.
[8] D.T.Scholes et al, Phys. Rev. C70(2004) 054314
[9] P.J. Nolan, Nucl. Phys. A520 (1990) 657c
[10] S.Aberg,Nucl.Phys.A520( 1990)350.
[11] J. Dobeezewski , ((Nuclear Structure98 Gatlinburg, AIP Conference Proceedings ))481(1998) 315
[12] J.dudek, Prog.Part.Nucl.Phys.28 (1992)131
[13] A.M. Khalaf, A. A. Zaki and A. M. Ismail, International Journal of Advanced Research in Physical Science 3 (2016) 21.
[14] W. Satula, R. Wyss and P. Magieaski, Nucl. Phys. A578 (1994) 45
[15] W. Satula and R. Wyss , Phys. Rev. C50 (1994) 2888
[16] B. Gall, et al , Z. Phys. A348 (1994) 1
[17] J. Terasaki, Nucl.Phys.A593 ( 1995)1
[18] J. Dobazewski and J. Dudex, Phys. Rev. C52 (1995)1827
[19] M.Girod, Phys. Lett. B325 (1994) 1
[20] A.Valor,J.L.Egido and L.M.Robledo,Phys.Lett. B392(1997)249.
[21] A.Villa France and J.L. Egido, Phys. Lett. B 403(1997) 35.
[22] A.V.Afanasjev , Phys. Rev. C60(1999) 051303 R
[23] J. Libert, M. Girod and J, P, Delaroche, Phys. Rev. C60 (1999) 054301
[24] Y.Sun, Jing –Ye -Zhang and M. Guidry, Phys. Rev. Lett.78 (1997) 2321.
[25] J.E. Draper et al, Phys. Rev. C42(1990)R1791.
[26] J.A. Becker et al, Nucl. Phys. A520 (1990) c187.
[27] J. Z. Zeng et al, Commun. Theor. Phys. 24 (1995) 125
[28] X.T. He et al ,Nucl. Phys. A760 (2005) 263
[29] A. M. Khalaf, M.A.Allam and M. M. Sirag. Egypt .J.Phys.41(2)(2010) 151
[30] A. Khalaf, M. Sirag and M. Taha, Turkish Journal of Physics TuBiTAK 37 (2013) 49
[31] A. M. Khalaf et al, Progress in Physics 3 (2013) 39
[32] A.M. Khalaf et al, International Joural of Theoretical & Applied Sciences, 7(2) (2015) 33.
[33] A.M. Khalaf, M. Kotb and K.E. Abdelmageed, Journal of Advances in Physics 6(3) (2014)1251.
[34] A. M. Khalaf and F.A. Altalhi, Journal of Advances in Physics 7(2) (2015) 1414
[35] A. M. Khalaf et al, Journal of Applied Physics (IOSR-JAP) 7 (5) (2015)1
[36] A. M. Khalaf, M. M. Sirag and M. A. Allam, Egypt .J. Phys 43 (1) (2015) 49
[37] A.M. Khalaf, and M. D. Okasha, Progress in Physics, 10(2014): 246.
[38] A.M. Khalaf, K.E. Abdelmageed and M. Sirag, Turkish Journal of Physics 39 (2015)178.
[39] A. M. Khalaf, T. M. Awwad and M. F. Elgabry, International Journal in Physical and Applied Sciences,3(4)(2016)47
[40] M.P. Carpenter et al, Phys. Rev. C51 (1995)2400.
[41] L.P. Farris et al, Phys. Rev. C51(1995)R2288.
[42] I.M. Hilbert et al, Phys. Rev. C54(199602253
[43] G. Hackmen et al, Phys. Rev. C55(1997)148.
[44] A.M. Khalaf, K.E. Abdelmageed andEman Saber, International Journal of Theoretical & Applied Sciences,6(2)(2014)56.
[45] A.M. Khalaf, H. Yassin and E.R. Aboelyazeed, Journal of Advances in Physics 11(1)(2015)2918.

[46] A.M. Khalaf, M.F. Elgabry and T.M. Awwad, International Journal Of Advanced Research in Physical Science (IJARPS) 2(12) (2015) 1.

[47] C.S.Wu and Z.N.Zhou,Phys. Rev. C56 (4),(1997)1814.

[48] A.M. Khalaf, M.D.Okasha and E.H.Ragheb, International Journal of Theoretical and Applied Science,8 ( 2) (2016)58

[49] A. Khalaf, M. Sirag and K.E. Abdelmageed, Chinese Journal of Physics 54(2016) 329

[50] A. M. Khalaf, Asma Abdelsalam and T.M. Awwad, International Journal in Physical & Applied Sciences,3(10)(2016)19.

[51] A. M. Khalaf, M. Kotb and T.M. Awwad , International Journal of Modern Physics E26 (2017) 1750011

## *التعرج في شركاء الدلائل للانوية فائقة التشوه في إطار نموذج الجسيم و الدوار*

**مديحة دسوقى عكاشة خليفة**

قسم الفيزياء – كلية العلوم (بنات)-جامعة الازهر

درست خمسة أزواج من شركاء الدلائل في منطقة رقم الكتلة ١٩٠و هما زئبق ١٩١ (حزم ٢و٣) و زئبق ١٩٣ (حزم ١و٢) و زئبق ١٩٣ (حزم ٣و٤) و ثاليوم ١٩١ (حزم ١و٢) و ثاليوم ١٩٣ (حزم ١و٢) في إطار نموذج الجسيم و الدوار .

افترضنا أن النواة مكونه من قلب مشوه متماثل محوريا و يحتوى عدد زوجي من البروتونات و النيوترونات مزدوج مع ثلاثة نيوكلونات تكافؤ .

افترض أن نيوكلونات التكافؤ تشغل مستويين من مدار دخيل ذو كمية تحرك زاوية عالية و مساقط $\frac{1}{2}$ ، $\frac{3}{2}$ .

تولدت دالتان أساسيتان استطعنا تقطير الهاملتونيان وإيجاد الطاقات التي تمثل القيم الذاتية و منها حسبنا الطاقات الانتقالية و التردد الدورانى و عزوم القصور الذاتية الكيناماتيكية و الديناميكية و التي تزايدت بزيادة التردد الدورانى وتطابقت النتائج النظرية مع المعطيات التجريبية مما أكد صلاحية النموذج المقترح .

فحصت ظاهرة التعرج في طاقات جاما الانتقالية لهذه الانوية رقم الكتلة الفردي وذلك باقتراح دالتان تظهر التعرج. الدالة الأولى تعتمد على الانتقال ثنائي القطب و رباعي الأقطاب بينما الدالة الثانية تعتمد على الانتقال ثنائي القطب فقط ، أظهرت النتائج سعات كبيرة في التعرج لجميع شركاء الدلائل.